Industrial Crops & Products 237 (2025) 122154

Contents lists available at ScienceDirect

Industrial Crops & Products

journal homepage: www.elsevier.com/locate/indcrop

Development and characterization of biobased sprayable mulches

Muhammad Ehtasham Akram [a], Brandi J. Brown [a], Mark Wilkins [b], Ozan N. Ciftci [a,c,*]

[a] Department of Biological Systems Engineering, University of Nebraska-Lincoln, Lincoln, NE 68583-0726, USA
[b] Carl and Melinda Helwig Department of Biological and Agricultural Engineering, Kansas State University, Manhattan, KS 66506, USA
[c] Department of Food Science and Technology, University of Nebraska-Lincoln, Lincoln, NE 68588-6205, USA

ARTICLE INFO

Keywords:
Bioplastic
Mulch
Biodegradable
Film
Sprayable
Chicken feather
Keratin
Waste

ABSTRACT

Polyethylene plastic mulch (PPM) films have been employed in high-value and specialty crop production as a physical barrier to weed growth since the 1950s. Over the last decade, due to the environmental problems associated with PPM, biodegradable plastic mulch (BPM) films have started to replace PPM films. However, concerns have arisen regarding the control of BPM film deposition, removal, and decomposition. Bio-based and biodegradable sprayable mulches are a promising substitute for BPM films. A series of biobased sprayable mulches (BSM) were developed using locally available biomaterials, including starch, protein, lignin, and chicken feather waste. Optimum BSM film-forming conditions of protein, starch, lignin, and glycerol mixtures were determined by evaluating different ratios. Keratin was isolated from chicken feathers by dissolving the feathers in a 1 M NaOH solution. The BSM film-forming solutions were physicochemically analyzed (pH, TDS, conductivity), transferred to petri dishes, and dried at 40 °C for 24 h. The dried BSM films were peeled from the petri dishes for mechanical testing, imaging, water absorption testing, and measuring mass loss percentage in water. BSM-12 exhibited the highest tensile strength (23 kPa), with an elongation at break of 15.39 % and a Young's modulus of 230 kPa. Finally, BSM-5 and BSM-12 film-forming solutions were suggested to assess their effectiveness in weed suppression and their impact on plant growth because of their higher tensile strength and elongation at break.

1. Introduction

Mulching is vital in agriculture as it decreases soil evaporation, inhibits weed growth, enhances soil water retention, and promotes crop development (Nan et al., 2016; Yin et al., 2018). Mulching can be performed with materials such as biodegradable film, liquid film, and crop residue. Of all the mulching materials, polyethylene is the most commonly used (Briassoulis, 2007; Horodytska et al., 2018; Picuno, 2014). Depending on the type of mulch employed, mulching conserves soil moisture and subsequently aids in establishing seedlings (Benigno et al., 2013; Woods et al., 2012) by minimizing soil exposure to direct sunlight. Mulching impacts soil organic matter through enhanced soil water retention and decomposition processes. Incorporating mulch leads to notable increases in soil carbon and nitrogen within the top 20 cm of soil (Youkhana and Idol, 2009). Organic mulches have a higher proportion of organic matter that integrates into the soil and enhances its qualities, including the number and activity of soil microbes (Chaparro et al., 2012; Huang et al., 2008).

Polyethylene mulching films offer advantages because of their easy handling, mechanical stability, and cost-effectiveness (Picuno, 2014). It has been reported that plastic films are widely used for mulching and cover an estimated 128,652 km^2 of agricultural land worldwide (Briassoulis and Giannoulis, 2018). The inability of plastic films to decompose naturally poses challenges for recycling and reuse, resulting in higher costs. Moreover, these mulches lead to rapid soil organic carbon degradation (Cuello et al., 2015). Furthermore, residues of plastic films harm soil structure, leading to deterioration of soil porosity and permeability (Zhang et al., 2019). As a result, exploring biobased and biodegradable soil mulches to replace plastic mulches and offering sustainable alternatives to PPM has become a prominent topic among researchers worldwide (Gloeb et al., 2023; Johnston et al., 2017).

Recent studies highlight polysaccharide-based mulch films, such as starch and cellulose composites, which improve soil health and crop yields while fully degrading in soil (Menossi et al., 2021). For example, polyester-coated paper mulches enable controlled fertilizer release, matching polyethylene's mechanical strength (Bi et al., 2021). Biochar-added bioplastics have shown efficacy in tomato cultivation, enhancing biodegradation and field performance (Malińska et al., 2022). High-hygroscopicity starch-based mulches facilitate plant

* Correspondence to: 264 Food Innovation Center, Lincoln, NE 68588-6205, USA.
E-mail address: ciftci@unl.edu (O.N. Ciftci).

https://doi.org/10.1016/j.indcrop.2025.122154
Received 7 August 2025; Received in revised form 12 October 2025; Accepted 19 October 2025
Available online 19 November 2025

Abbreviations

BSM	Biobased Sprayable Mulch
PPM	Polyethylene Plastic Mulch
BPM	Biodegradable Plastic Mulch
CFW	Chicken Feather Waste
CFKH	Chicken Feather Keratin Hydrolysate
CS	Corn Starch
CZ	Corn Zein
ISP	Isolated Soy Protein
PP	Pea Protein
PS	Potato Starch
KL	Kraft Lignin
TDS	Total Dissolved Solids
WA	Water Absorbency
MW	Mass Loss in Water
FTIR	Fourier Transform Infrared
TGA	Thermogravimetric Analysis
SEM	Scanning Electron Microscopy
TKP	Total Kjeldahl Phosphorus
TS	Tensile Strength
EB	Elongation at Break
YM	Young's Modulus

growth by improving soil moisture retention (Chen et al., 2020), while protein-based sprayable coatings offer scalable application methods (Schettini et al., 2012). Meta-analyses confirm biodegradable mulches' comparable performance to polyethylene in weed suppression and yield, though long-term soil impacts require further study (Tofanelli and Wortman, 2020). Life cycle assessments emphasize lower environmental footprints for soil-biodegradable mulches, but challenges remain in optimizing degradation rates and nutrient integration (Dada et al., 2025; Ferreira-Filipe et al., 2021). Biodegradable mulches also influence soil microbial communities, supporting ecosystem health (Serrano-Ruiz et al., 2021). Nitrogen release from biodegradable films enhances plant-soil systems, particularly in nutrient-poor soils (Wang et al., 2022). Unlike these studies, which focus on pre-formed films or higher-cost materials, this study develops sprayable mulches from low-cost CS and CFW-derived keratin, achieving mulching and high nitrogen content for dual weed suppression and soil enrichment.

Proteins, cellulose, and alginic acid are commonly used as primary components in developing mulches for agricultural applications due to their biodegradable nature. Nonetheless, starch has attracted considerable interest as a promising material for soil mulches. Starch is a naturally occurring biodegradable polymer obtained from various plant sources such as corn, wheat, rice, potatoes, and peas (Benito-González et al., 2019; Gloeb et al., 2023). Starch is abundantly available and cost-effective compared to cellulose and protein, with a simpler pretreatment method. Typically, starch solutions undergo gelatinization at temperatures of approximately 85–90 °C to disrupt their crystalline structure. However, these solutions become unstable and form gels upon cooling, a phenomenon known as retrogradation. This retrogradation occurs because of the association of glucose units within the starch molecules (Wang et al., 2015). The primary crystalline component of starch is the short branching chains found in amylopectin (Li et al., 2019). However, bioplastics composed solely of starch are widely recognized for their inherent fragility (Briassoulis, 2006). Furthermore, these starch-based bioplastics exhibit inadequate water resistance, low moisture retention capacity, and unsatisfactory hygroscopic properties (Briassoulis, 2007). Starch-based bioplastics can be produced through thermal film-forming processes and the casting method (Sabatino et al., 2018). These manufacturing techniques have significantly higher labor and disposal costs than sprayable mulching materials (Gloeb et al., 2023; Schettini et al., 2012).

In recent years, sustainable and eco-friendly materials have gained significant importance in various fields, including agriculture. This trend is driven by the pivotal role of biocomposites in fabricating novel eco-friendly materials across diverse applications, such as food packaging, chemical processes, and separations. For instance, Maillard reaction-based glycation enhances the properties of biopolymeric packaging films through non-enzymatic browning, improving mechanical properties, barrier functions and ultimately food shelf life (Zhang et al., 2023). Similarly, gelatin-chitosan interactions in edible films doped with plant extracts enable preservation of perishable products like tuna, leveraging antimicrobial and antioxidant properties (Eranda et al., 2024). Recent advances in reinforced bioplastics for food packaging highlight the use of fillers to boost mechanical strength and biodegradability (Siddiqui et al., 2024). Arabinoxylans, recovered from cereal byproducts, serve as functional ingredients in food formulations, offering prebiotic benefits and improved texture (Hernández-Pinto et al., 2024). Chitosan-based electrospun nanofibers encapsulate bioactive ingredients, enhancing controlled release in functional foods (Castro-Muñoz et al., 2023). These developments underscore the shift toward sustainable biomaterials. Building on this, one promising material for agricultural applications, such as mulching, is chicken feather waste (CFW).

Keratin, naturally found in chicken feathers, is a fibrous protein that is promising for bioplastic applications (Ramakrishnan et al., 2018). Approximately 90 % of chicken feathers' composition is keratin, which can be used as an ingredient in bioplastic. However, to utilize this keratin, the feathers must be subjected to hydrolysis to break down peptide bonds and release keratin from the rigid feather structure (Virtanen et al., 2017). According to the United States Department of Agriculture (USDA), approximately 2.75 billion kg of chicken feathers are generated annually in the US. These feathers are usually disposed of in landfills, creating environmental problems. However, utilizing CFW as a mulching material can address both CFW disposal issues and offer an eco-friendly alternative to non-biodegradable mulching materials. Furthermore, CFW is abundant in nitrogen, which can enrich soil fertility and enhance crop productivity (Gloeb et al., 2023). In this context, our study focuses on developing BSMs from starch-keratin hydrolysates derived from CFW, aiming to provide a biodegradable alternative to PPM with enhanced mechanical properties and nutrient release for agricultural applications.

Building on these foundations, this study aims to develop and characterize BSM formulations for potential agricultural applications. Corn starch (CS) and keratin extracted from CFW were used as primary components, while corn zein (CZ) and isolated soy protein (ISP) were incorporated to enhance weed suppression performance. Additional biopolymers, including pea protein (PP), potato starch (PS), and kraft lignin (KL), were included for comparative purposes. Based on mechanical property assessments, two formulations demonstrating optimal performance were selected for further evaluation of their weed-suppressing efficacy under both greenhouse and open field conditions.

2. Materials and methods

2.1. Materials

CS containing 28 % amylose and 72 % amylopectin, NaOH pure pellets, glycerin (ACS grade, liquid), and CZ (purified) were purchased from Thermo Fisher Scientific (Waltham, MA, USA). PS containing 18 % amylose and 82 % amylopectin was from Spectrum Chemical (New Brunswick, NJ, USA), ISP from MP Biomedicals (Irvine, CA, USA), PP from Newark Nut Company (Newark, NJ, USA), and KL was from Tokyo Chemical Industry (Portland, OR, USA). CFW was provided by Smart

Table 1
Composition of the various biobased sprayable mulch (BSM) formulations.

Form #	KH (% V/V)	CS (% W/V)	CZ (% W/V)	ISP (%W/V)	Gly (% V/V)	PP (% W/V)	PS (% W/V)	Lignin (%W/V)
1	75	8	2.03	2.03	18.94	-	-	-
2	76	7	1.98	1.98	18.47	-	-	-
3	79	5	2.03	2.03	15.10	-	-	-
4	75	5	2.03	2.03	18.94	-	-	-
5	75	4	2.03	2.03	18.94	-	-	-
6	75	-	2.03	2.03	18.94	-	4	-
7	75	2	2.03	2.03	18.94	-	2	-
8	75	4	2.03	-	18.94	2.03	-	-
9	75	4	2.03	2.03	18.94	-	-	0.30
10	75	4	2.03	2.03	18.94	-	-	0.60
11	75	4	2.03	2.03	18.94	-	-	0.90
12	73	4	1.98	1.98	18.47	-	-	1.50

KH: Keratin Hydrolysate; CS: Corn Starch; CZ: Corn Zein; ISP: Isolated Soy Protein; Gly: Glycerol; PP: Pea Protein; PS: Potato Starch.

Chicken (Waverly, NE, USA). Ethanol was purchased from Decon Labs, Inc. (King of Prussia, PA, USA). All chemicals utilized were of analytical grade and were used without additional purification.

2.2. Obtaining keratin from chicken feathers

2.2.1. Pretreating chicken feathers

CFW underwent pretreatment to remove lipid compounds and other impurities, and to improve hydrolysis yield. Initially, it was washed thoroughly with warm water and detergent until both lipids and impurities were removed. Then, it was washed with ethanol to eliminate bacteria and other contaminants. Finally, it was washed with detergent once more, dried at 50 °C for 24 h, and stored in plastic bags for future use.

2.2.2. Alkaline hydrolysis of chicken feathers

The hydrolysis process was carried out at room temperature to avoid excessive breakdown of peptide bonds and to ensure the retention of high molecular weight protein fractions (Mokrejs et al., 2011). The treated feathers were introduced into a 1 M NaOH solution (Dąbrowska et al., 2022). The ratio of the volume of 1 M NaOH to the weight of the feathers was established at 100:3 (v/w), and the mixture was stirred for 72 h. The obtained hydrolysate was centrifuged at 10,000 rpm for 15 min to separate and remove any insoluble feather residues. The centrifuged chicken feather keratin hydrolysate (CFKH) was neutralized with 18 M H_2SO_4 and stored at 4 °C in the refrigerator until needed.

2.3. Preparation of BSM formulations

CS was added to CFKH, homogenized for 2 min, heated to 85°C for 30 min, and subsequently brought to a boil on a hot plate while continuously stirring using a magnetic stirrer. Protein from various sources listed in Table 1 was thoroughly mixed with glycerol in a separate beaker. This protein-glycerol mixture was added to the boiling starch solution while continuously stirring with a magnetic stirrer for 10 min. Finally, each variation was poured into petri dishes and dried at 40 °C for 24 h in an oven. The concentrations of the various components in each formulation are displayed in Table 1.

2.4. Properties of the BSM formulations

2.4.1. Viscosity

The viscosity of each formulation was assessed using an Anton-Paar Physica MCR 301 Digital Rheometer (Houston, TX, USA). A zero-gap setting of 0.5 mm was established. All samples were evaluated at 25 °C following a 150 s equilibration period. Viscosity assessments were performed across shear rates ranging from 0.1 to 1000 s^{-1}. The viscosity versus shear rate relationship (flow curve) was documented.

2.4.2. Physicochemical characterization

Initially, a series of physicochemical parameters, which included pH, total dissolved solids (TDS) (measured in ppm), and conductivity (measured in μS/cm), were assessed in each formulation using an elite PCTS tester (Thermo Fisher Scientific). The tester offers ± 0.01 accuracy for pH measurements and ± 1 % for conductivity and TDS.

2.5. Surface color and appearance of bioplastics

The behavior of bioplastics in terms of surface cracking, stickiness, brittleness, and ease in peeling was observed. The color of the sample surface was determined using a CR-300 Chroma Meter (Minolta Chroma Meter CR-300, Minolta Co. Ltd, Japan). The Chroma Meter was calibrated to conform to the standard colors specified in the setup. Three measurements were taken for each film sample by assessing it at three randomly chosen locations, one of which was the center. The L* a* b* values were analyzed to determine the brightness and color of each sample.

2.6. Mechanical properties

The films were removed from the petri dishes and cut into 20 mm wide and 40 mm long specimens. Tensile strength, breaking elongation, and Young's modulus of the films were evaluated by ASTM D882 standards. These films had an average thickness of 0.25–0.30 mm. Before the tests, all samples were conditioned for at least 72 h at 21 °C and 65 % relative humidity. Tensile testing utilized a universal material tester (MTS Qtest 10, MN, USA) fitted with a 500 N load cell.

2.7. Water absorbency and mass loss in water

Water absorbency (WA) and mass loss in water (MW) were determined using the method given by Chen et al. (2020) and Qin et al. (2024) with slight modifications. The sample was cut into 4 × 3.5 cm specimens and dried to a stable weight in an oven at 100 °C. The weight was recorded as m_0 (g). The dried sample was soaked in distilled water for 24 h at ambient temperature (25 ± 2 °C) to achieve full swelling. After 24 h, surplus water from the swollen sample was decanted, then removed entirely from the surface using tissue paper, and the weight was recorded as m_1 (g). Then, the swollen sample was re-dried in an oven at 100 °C until a stable weight was attained, and the sample weight was noted as m_2 (g). WA (g/g) values were computed using Eq. (1), and MW (%) values were determined using Eq. (2).

$$WA\ (g/g) = m_1/m_0 \quad (1)$$

$$MW\ (\%) = [m_0 - m_2/m_0] \times 100 \quad (2)$$

2.8. Characterization of the bioplastic samples

The samples that exhibited the most favorable outcomes in making stable bioplastic, mechanical properties, WA, and MW were chosen for additional characterizations as described below.

2.8.1. Fourier transform infrared (FTIR) spectroscopy

The chemical structure of BSM films was characterized using an FTIR spectrometer (Nicolet AVATAR 380 FT-IR). The spectral data were recorded over the 4000–500 cm^{-1} wavelength span.

2.8.2. Thermal stability

The thermal stability of the BSM samples was investigated through thermogravimetric analysis (TGA) using a TA Instruments TGA550. The

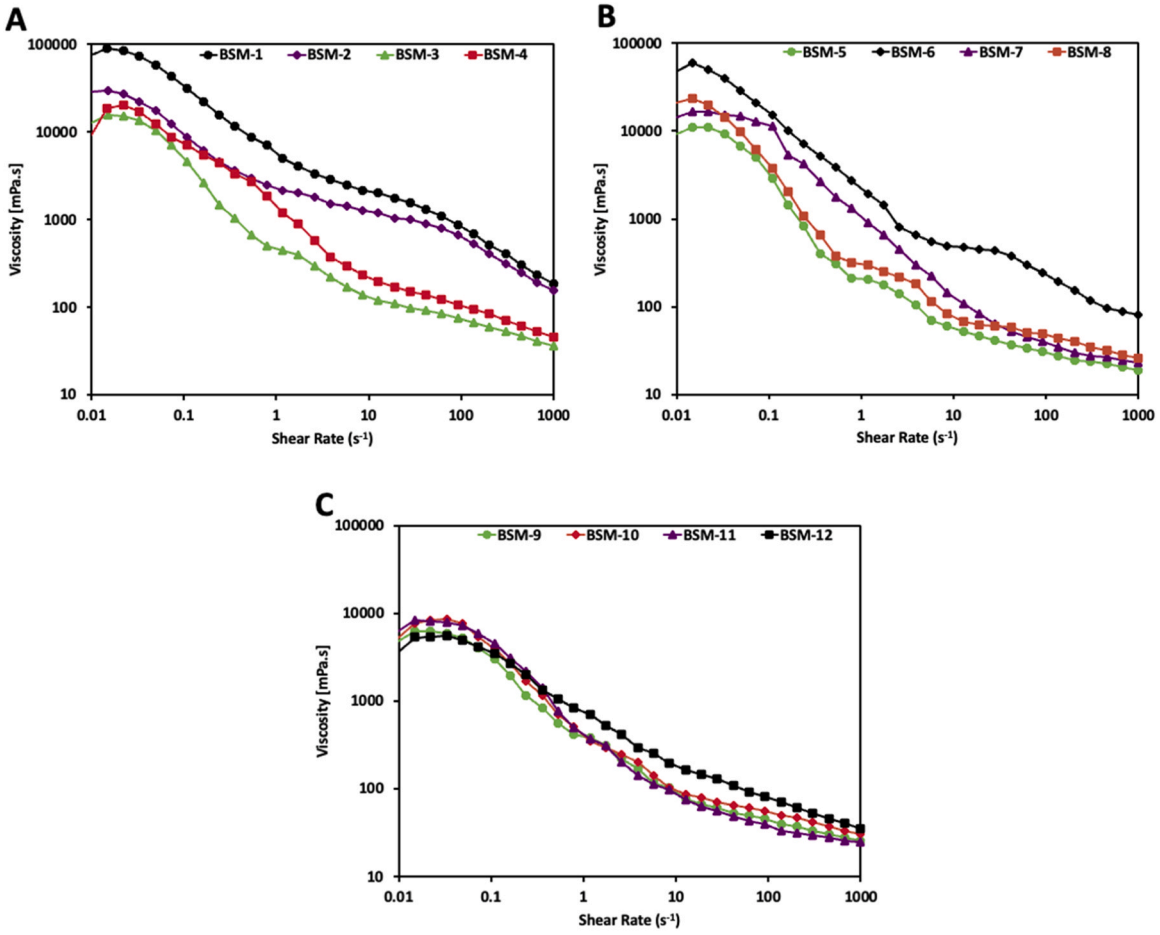

Fig. 1. The viscosity of film forming solutions at 25 °C. (A) Formulations 1–4; (B) Formulations 5–8; (C) Formulations 9–12.

test involved varying the temperature from 25 to 600 °C at a constant heating rate of 10°C/min. Film samples weighing approximately 10–15 mg were loaded into aluminum stubs and subjected to heating, with the resulting weight reduction versus temperature profile recorded.

2.8.3. Morphology

Scanning electron microscopy (SEM) was performed with a Hitachi microscope (S4700 Field-Emission) for surface morphology examination of BSM films. Images were captured using an excitation voltage of 5.0 kV and at varying magnification levels. Preceding the SEM analysis, the specimens were attached to aluminum stubs and coated with a thin layer of chromium metal to avoid charging. The coating thickness was approximately 2–5 nm.

2.8.4. Percentage of carbon and nitrogen

The quantities of organic carbon and nitrogen were determined through flash combustion using a Carlo Erba NA 1500 Series 2 elemental analyzer. Samples were finely ground, weighed into tin capsules, and dropped into a heated reactor. Gaseous combustion products were oxidized and reduced under a stream of helium before being separated on a chromatographic column. A thermal conductivity detector (TCD) was employed to detect the gases. Detector response was calibrated with standard reference samples, and results were expressed as %C and %N.

2.8.5. Total Kjeldahl phosphorus

Measurement of Total Kjeldahl Phosphorus (TKP), which includes organic and inorganic P, used a copper catalyst (Standard Methods 4500-N B and C which conforms to EPA method 351.2), followed by colorimetric analysis of orthophosphate on a Seal AQ2 Discrete Analyzer (SEAL Analytical Inc., Mequon WI) and by EPA Method 365.4. (Method 365.4: Phosphorous, Total (Colorimetric, Automated, Block Digester AA II), n.d.). Results were reported in total P (μg/g).

2.8.6. Nitrate-N and ammonia-N

Extractable reactive nitrogen (nitrate and ammonia-N) was determined in samples using a Lachat Quikchem 8500 Flow Injection Analysis (FIA) analyzer (Hach, Loveland, CO) (QuikChem Methods 12-107-04-1-B and 12-107-06–3-B). Samples were extracted using a 1 M KCl solution, and concentrations were expressed as nitrate-N and ammonia-N in μg/g (Spalding and Kitchen, 1988).

3. Results and discussion

3.1. Viscosity

The viscosity of the BSM needed to be sufficiently low so that the material could smoothly flow through a small nozzle and be sprayed. Fig. 1 illustrates a decrease in the apparent viscosity of the formulations at 25 °C as the shear rate increased, indicating the pseudoplastic nature of the formulations and their tendency toward shear-thinning. The apparent viscosity and shear rate were presented on a logarithmic scale for effective comparisons. Starch played a leading role in the formulations, outweighing the contributions of other ingredients. Apparent viscosity of the formulations increased directly with the increase in starch concentration. The formulation containing 8 % CS exhibited the highest peak apparent viscosity, reaching 75,584 mPa·s at a shear rate of 0.01 s^{-1}. In comparison, a systematic reduction in viscosity was observed as the starch content was reduced to 4 %. This trend was

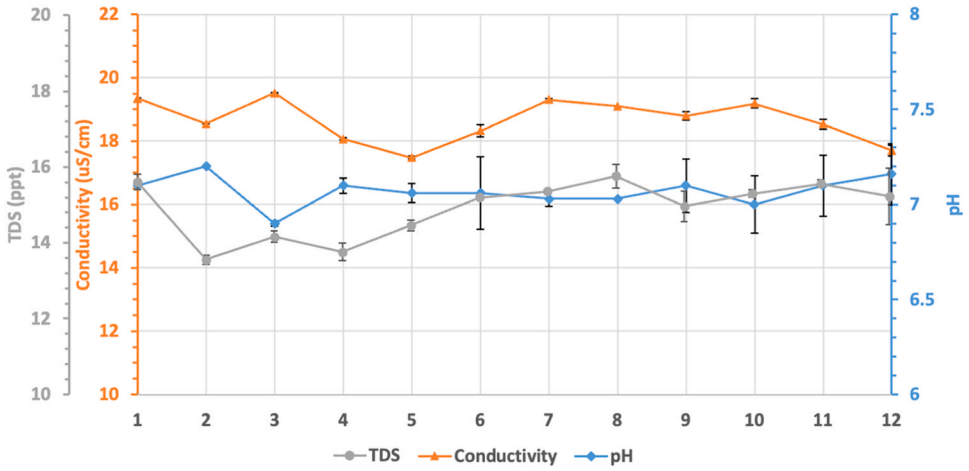

Fig. 2. pH, conductivity, and TDS of the film forming solutions.

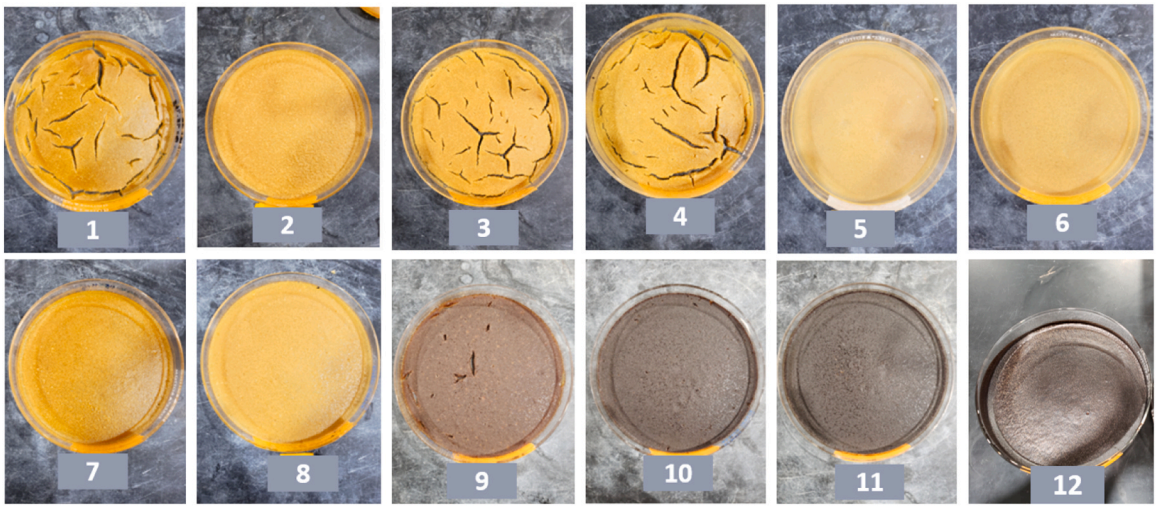

Fig. 3. Photos of the developed BSM.

consistent with expectations, as apparent viscosity correlates directly with the starch quantity (Santamaria et al., 2021).

However, the introduction of lignin reduced the viscosity of the film-forming solutions compared to other formulations (Fig. 1C). This decrease implies that lignin worked as a lubricating agent (Zadeh et al., 2018). When the concentration of lignin increased, the viscosity decreased, which was attributed to the formation of intermolecular secondary bonds between starch and lignin.

3.2. Physicochemical characterization of film-forming solutions

The film forming solutions obtained from different compositions as detailed in Table 1 were evaluated for pH, conductivity, and TDS (Fig. 2). The film forming solution's pH neither changed by using starch and protein from different sources nor by adding lignin into the system, ranging from 6.9 to 7.2. Hence, it could be concluded that the pH values of the film-forming solutions, using different protein and starch sources, were within the allowed range for agricultural use (pH 6.5–7.5), ensuring compatibility with soil microbial activity and crop growth requirements (Serrano-Ruiz et al., 2021).

Apart from pH, the film-forming solutions were assessed for TDS and conductivity to determine their electrical conductivity and the number of dissolved solids they contained. Fig. 2 shows that the TDS values fell within the range of 11.7–15.8 ppt, while the conductivity values ranged from 17.45 to 19.51 μS/cm.

3.3. Surface color and appearance of bioplastics

The developed BSM films are visually represented in Fig. 3, and visual attributes are detailed in Table 2. The BSM films showed rigidity, brittleness, and fragility, which can be due to their higher starch levels. Due to this high starch concentration, the films tended to break into small fragments, making both peeling and handling challenging. The observed fragility and stiffness of the surface broken films were attributed to numerous starch-starch chain molecules within the material. Azahari et al. (2011) reported that, as the amount of starch increased, the filler-filler interaction became more prominent, resulting in a decrease in the strength of the material. The maximum amount of CS for bioplastic formation in the current study was 4 %. A concentration greater than 4 % increased filler-filler interaction, leading to a decrease in the material's strength. These findings align with the observations made by Suppakul et al. (2013) and Talja et al. (2007) who had previously worked on starch-based biopolymers using cassava starch and potato starch, respectively.

Color is a significant parameter for mulches because different colors influence the soil's hydrothermal environment, weed suppression, and crop growth due to their unique optical attributes (Sokombela et al., 2025; Yin et al., 2018). In the evaluation of biopolymer-based films,

Table 2
Color parameters of BSM bioplastic.

BSM sample	Color parameter			Appearance
	L*	a*	b*	
1	98.09 ± 1.50^{ab}	0.19 ± 0.08 ^{cd}	2.24 ± 0.65 ^{cd}	The material was rigid, fractured into small fragments, and could not be peeled.
2	89.25 ± 0.25^{d}	− 0.56 ± 1.31^{de}	13.36 ± 0.51^{b}	The material was rigid, fractured into small fragments, and could not be peeled.
3	93.93 ± 0.62^{c}	− 1.38 ± 0.07^{e}	18.45 ± 1.20^{a}	The material extensively cracked into numerous pieces, was highly brittle, rigid, and could not be peeled.
4	93.74 ± 1.29^{c}	− 1.36 ± 0.14^{e}	17.14 ± 3.50^{a}	The material was rigid, brittle exhibited wide cracks and could not be peeled.
5	99.13 ± 0.74^{ab}	2.73 ± 0.14^{a}	− 4.77 ± 0.74 ^{f}	The surface was free from cracks, and the material was neither brittle nor fragile. It was flexible, exhibited a slight stickiness, and could be easily peeled.
6	97.75 ± 0.61^{ab}	− 0.29 ± 0.07^{de}	− 1.18 ± 0.06^{e}	The surface was free from cracks, and the material was neither brittle nor fragile. It was flexible, exhibited a slight stickiness, and could be easily peeled.
7	99.40 ± 0.79^{a}	0.13 ± 0.08 ^{cd}	0.72 ± 0.39^{cde}	The surface was free from cracks, and the material was neither brittle nor fragile. It was flexible, exhibited a slight stickiness, and could be easily peeled.
8	97.24 ± 0.39^{b}	− 0.24 ± 0.05^{de}	− 1.01 ± 0.02^{de}	The surface was free from cracks, and the material was neither brittle nor fragile. It was flexible, exhibited a slight stickiness, and could be easily peeled.
9	24.66 ± 0.41^{e}	1.39 ± 0.08^{b}	3.32 ± 0.23^{c}	The surface was free from cracks, and the material was neither brittle nor fragile. It was flexible, exhibited a slight stickiness, and could be easily peeled.
10	24.44 ± 0.21^{e}	0.42 ± 0.12^{bcd}	1.74 ± 0.02^{cde}	The surface was free of cracks, and it was neither brittle nor fragile. It had flexibility, possessed a mild stickiness, and could be easily peeled.
11	24.05 ± 0.24^{e}	0.25 ± 0.11^{bcd}	1.23 ± 0.05^{cde}	The surface was free of cracks, and it was neither brittle nor fragile. It had flexibility, possessed a mild stickiness, and could be peeled easily.
12	23.26 ± 0.10^{e}	1.17 ± 0.08^{bc}	2.74 ± 0.07^{c}	The surface was free of cracks, and it was neither brittle nor fragile. It had flexibility, possessed a mild stickiness, and could be peeled easily.

Same letters within a column indicates no significant differences ($P > 0.05$).

three color parameters, namely, L* (lightness), a* (red/green), and b* (yellow/blue), are reported.

The color parameters of BSM films produced with and without lignin are recorded in Table 1. The results indicated that the inclusion of lignin in BSM films led to a reduction in the brightness of the films. This decrease was due to the inherent dark brown color of lignin. Increasing the lignin content did not affect the L-value significantly, as could be observed from the table. Rising a* values signify a shift towards a reddish hue in the films, whereas increasing b* values indicate a more pronounced yellow color in the films.

3.4. Mechanical properties

Biopolymer films are primarily characterized by their mechanical properties, encompassing TS, EB, and YM. These mechanical properties provide insights into the film's integrity under stressful conditions. TS reflects the film's strength and is determined by dividing the maximum force required to fracture the films by their cross-sectional area; whereas, EB indicates film's flexibility and YM serves as an indicator of the film's stiffness (Amin et al., 2019; Bhat et al., 2013). Research highlights that the mechanical characteristics of PPM and biodegradable extruded films differ significantly from those of BSMs (Immirzi et al., 2009).

The formulations BSM-1, BSM-2, BSM-3, and BSM-4 did not result in stable, peelable bioplastics due to their high percentage of CS (over 4 %), thus they could not be tested for mechanical properties. Films from the other 8 formulations were tested for mechanical properties. TS values of the BSM films were in the range of 11–23 kPa (Fig. 4A). The highest TS was observed for BSM-12 being 23 kPa followed by BSM-11 with TS value of 22.3 kPa, these were not significantly different than each other. An increase in lignin content from 0.3 % to 1.5 % in BSM-10, BSM-11, and BSM-12 formulations resulted in a progressive enhancement of TS, likely due to improved intermolecular interactions within the polymer matrix. The TS of the BSM films was much less than what was observed in previous studies on starch-based bioplastics. A previous study stated that starch-based bioplastics when grafted with acrylic acid had TS of 6.10 MPa, and EB of 5.4 % (Chen et al., 2020). In another study the TS of CS and PS based films were 2.21 MPa and 3.16 MPa, respectively (Datta and Halder, 2019).

TS of casted films is heavily dependent on both water content and eventual film thickness. Additionally, the mechanical attributes of films are significantly impacted by the quantities of plasticizer and water used in the film preparation process (Basiak et al., 2017). The film formation properties, gelation properties, and the crystalline structure of the films are substantially determined by the content of amylose and amylopectin, as well as structural variations inherent to each type of starch (Torres et al., 2011); thereby, this variation results in differences in the TS and EB of the biofilms derived from various starch sources (Mali et al., 2006). CS films had a mean TS of 17.7 kPa while BSM-6 had a TS of 15 kPa, which may be due to the lower amylose content in PS (21 %) compared to CS (28 %) (Fig. 4A). The TS of 1:1 PS:CS (BSM-7) film was 11 kPa. The high TS of PPM is crucial for the mechanical application and removal of PPM films, a requirement not applicable to BSMs, as noted by Adhikari et al. (2016).

In Fig. 4B, the highest EB was observed in BSM-5 and BSM-8. Conversely, BSM-6 and BSM-7 exhibited the lowest EB. Regarding YM, BSM-5 exhibited the lowest value, while BSM-12 displayed the highest value (Fig. 4C). Notably, there were no significant differences in YM among BSM-9, BSM-10, and BSM-11, which could be attributed to the marginal increase in the amount of lignin in each variant.

3.5. Water absorbency (WA) and mass loss in water (MW)

In Fig. 5A, WA values of BSM films showed a decreasing trend (from 1.18 to 1.07 g/g) with the addition of lignin. The WA values of BSM-9 (1.18 g/g) to BSM-12 (1.07 g/g) were similar, mainly due to the small difference in the amount of lignin added to each variant. WA values for films with lignin were smaller than BSM films without lignin. This decrease could be attributed to hydrophobic aromatic groups in the chemical structure of lignin. When lignin is incorporated into bioplastics, it contributes to the overall hydrophobicity of the material, thereby reducing WA and enhancing water resistance. MW reflects the

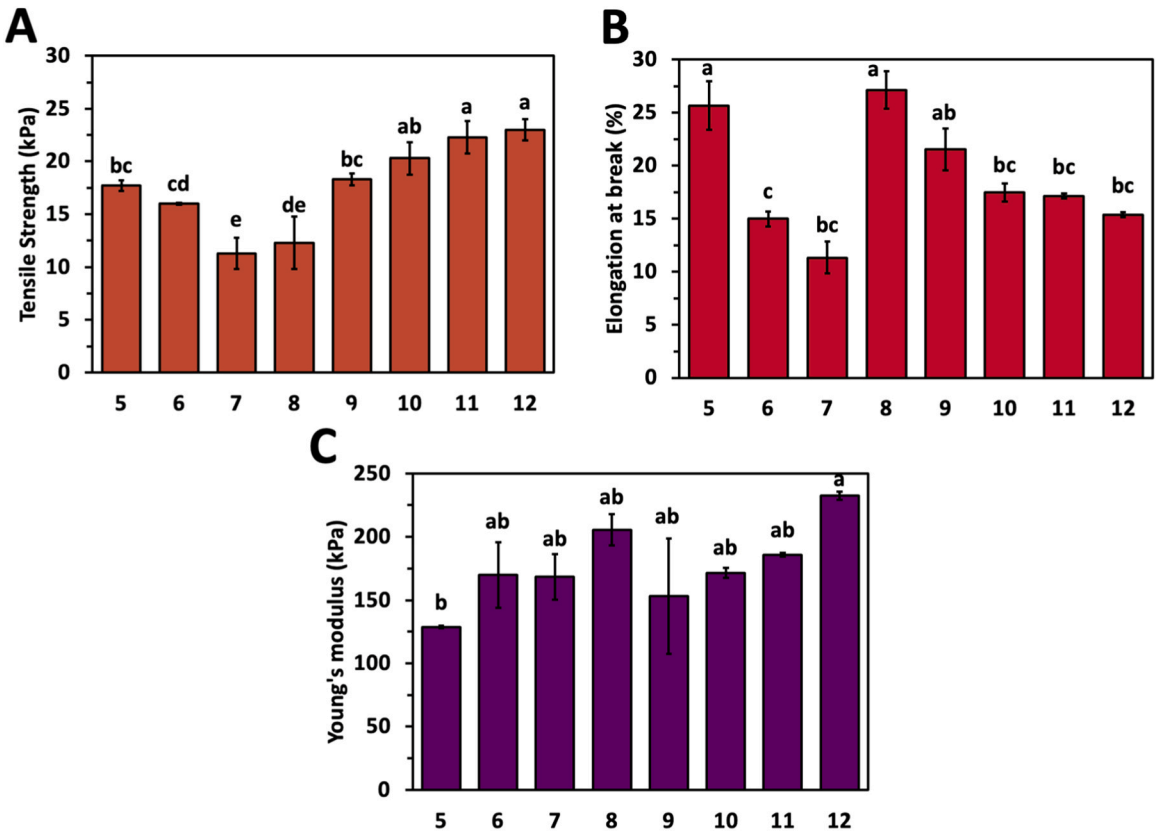

Fig. 4. Mechanical properties of different composition films. (A) tensile strength, (B) elongation at break, and (C) Young's modulus. Graph represents mean ± SD followed by same letter is not significantly different at $p \leq 0.05$.

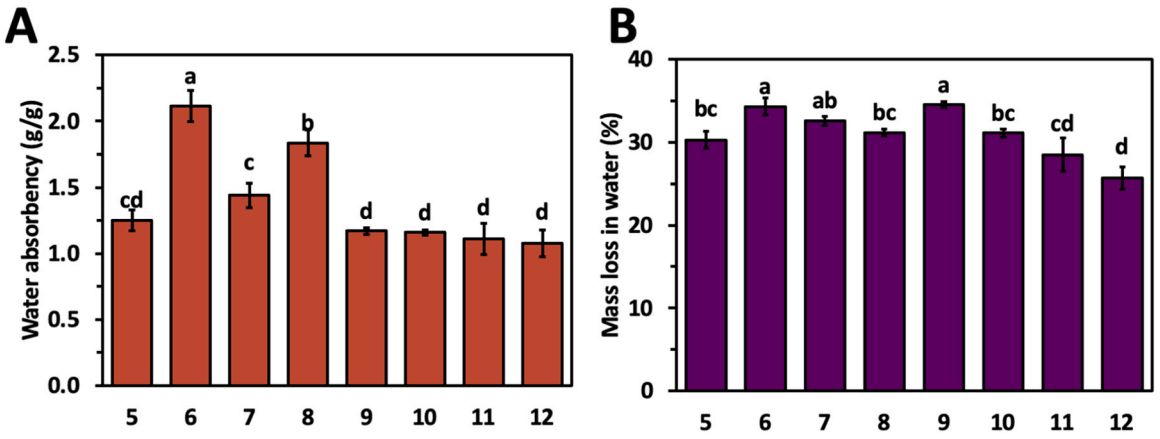

Fig. 5. Water absorbency and mass loss in water performance of different composition films. (A) water absorbency, (B) mass loss in water. Graph represents mean ± SD followed by same letter is not significantly different at $p \leq 0.05$.

water-resistant properties of BSM films. Fig. 5b illustrates that the addition of lignin resulted in a decrease in MW values from 34.89 % to 27.23 % (BSM-9 to BSM-12). The decrease in MW values can be explained by the increase in lignin concentration, leading to a more hydrophobic network structure in BSM, consequently, the MW values of the BSM films gradually decreased. These findings represented the behavior of BSM films in water, as the water absorbency (WA) and mass loss in water (MW) are critical for retaining soil moisture and stabilizing temperature variations due to water's high specific heat capacity as reported by Qin et al. (2024).

3.6. Fourier transform infrared (FTIR) spectroscopy

Fig. 6a and b display the IR spectra of BSM bioplastics. From these figures, it was evident that all the films exhibited similar characteristics. Broad bands within the 3200–3300 cm^{-1} range were identified in all the films, indicating the stretching vibrations of O–H groups in starch and glycerol (Lorenzo Santiago et al., 2024; Kurt and Kahyaoglu, 2014; Nordin et al., 2020; Tongdeesoontorn et al., 2012). The peaks of 2934 and 2935 cm^{-1} were ascribed to the (C–H) methyl group, as reported by Edhirej et al. (2017) and Nordin et al. (2020). A notable absorption peak within the 1637–1647 cm^{-1} range was linked to the presence of hydroxyl groups within the starch films, which had absorbed water (Park

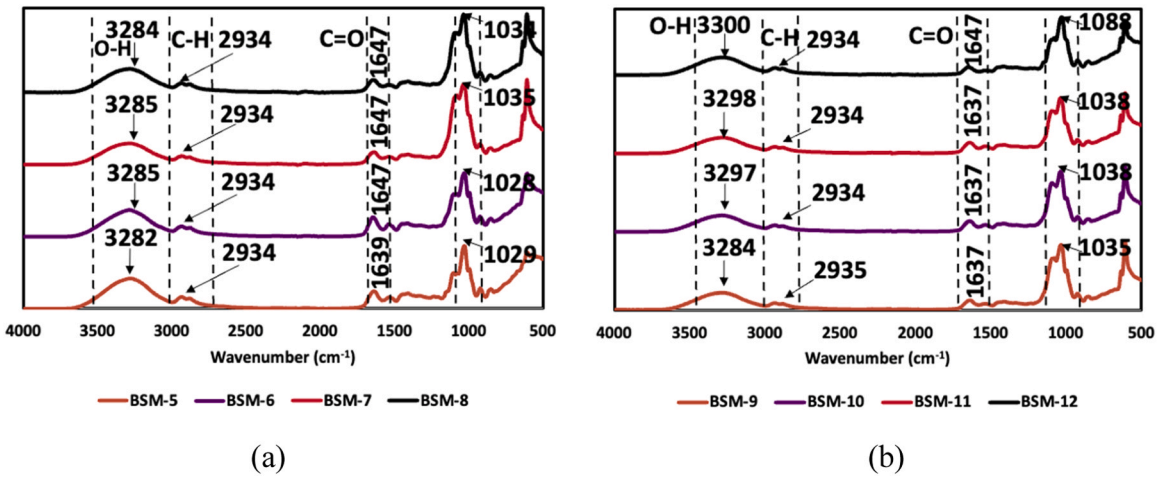

Fig. 6. FTIR spectra of different composition films (a) BSM-5, BSM-6, BSM-7, and BSM-8, (b) BSM-9, BSM-10, BSM-11, and BSM-12.

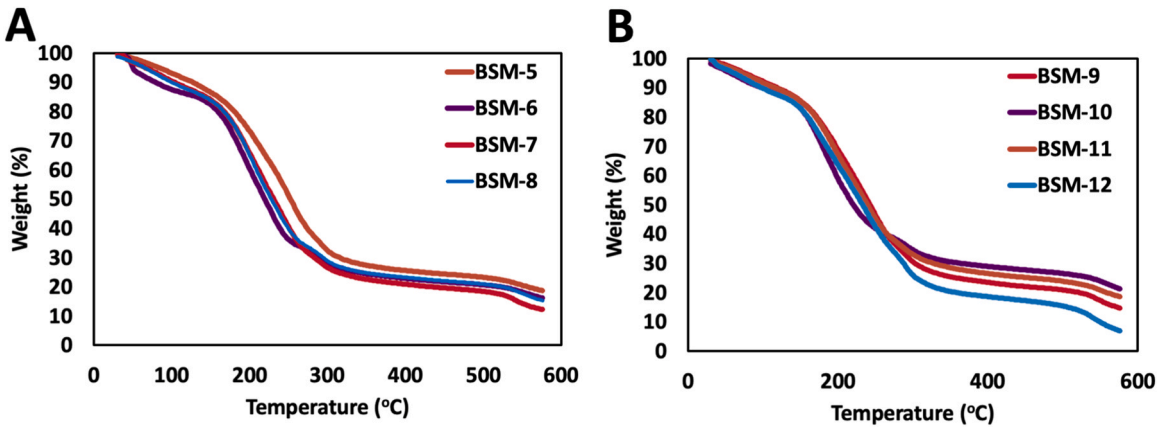

Fig. 7. TGA curves of different composition films (A) BSM-5, BSM-6, BSM-7, and BSM-8, (B) BSM-9, BSM-10, BSM-11, and BSM-12.

et al., 2000; Sahari et al., 2014). This peak might also be associated with the O–H stretching vibration groups in glycerol, which functions as a plasticizer.

Furthermore, the absorption bands at 1030 cm^{-1} and 1038 cm^{-1} resulted from C–O(H) and C–O–C functional groups, respectively. FTIR analysis indicated that the films' chemical structure remained predominantly unchanged even after lignin was incorporated into the composition. The stability of the molecular structures in the resulting films was evident, as no significant chemical reactions were attributed to the presence of lignin.

3.7. Thermal stability

Thermogravimetric analysis (TGA) assessed the bioplastic film's thermal degradation and stability. The percentage of film decomposition in relation to temperature is presented in Fig. 7a and b. The TGA curves revealed a triphasic thermal degradation process in the films. This trio of thermal decomposition stages observed in most starch-based films has been previously reported (Dang and Yoksan, 2015; Sanyang et al., 2015). The temperature ranges for the three steps were 70–110 °C, 110–200 °C, and 200–330 °C. These temperature intervals were associated with specific processes; the first step corresponded to evaporation of free water (Pelissari et al., 2009), the second step involved the evaporation of bound water and glycerol (Cyras et al., 2008), and the third step was linked to the breakdown of starch (Pelissari et al., 2009). Similar observations were made in biodegradable carbon-ashes and CS-based composite mulches by Stasi et al. (2020).

Including lignin resulted in a more pronounced weight reduction in the film, which diminished as the lignin content increased. For instance, at 300 °C, the total weight loss for BSM-9, BSM-10, BSM-11, and BSM-12 films was 35.7 %, 34.5 %, 33.0 %, and 25.9 %, respectively. Following decomposition at 350 °C, the BSM-12 film exhibited the lowest remaining weight, while the other films retained a higher weight. Nevertheless, the decomposition temperature (Td) of the BSM film exhibited minimal variation with lignin addition and was approximately 360 °C.

3.8. Morphology

Fig. 8 shows the surface and cross-section morphologies of the resulting films. Decreasing the percentage of starch in the formulation made the surface less porous and rough. Furthermore, the starch ratio strongly affected the presence of pores in the structure. The structures of BSM-1 to BSM-4 films were more heterogeneous and showed many structural irregularities and pores, while the BSM-5 film showed a lower number of pores and interstices. Moreover, this also agrees with mechanical properties already reported, as the BSM-5 with 4 % CS bioplastic possessed higher TS, supported by a more compact structure, with a lower porosity. Adding PS made a coarse structure as opposed to CS, while adding 2 % CS with 2 % PS made a grainy structure as observed in BSM-7. BSM-8 film was made with PP instead of ISP. This film could be observed to bear a grainy structure due to PP's lower solubility than ISP. When lignin was added to the formulations, the films had a rough and coarse structure with many holes. This structure could

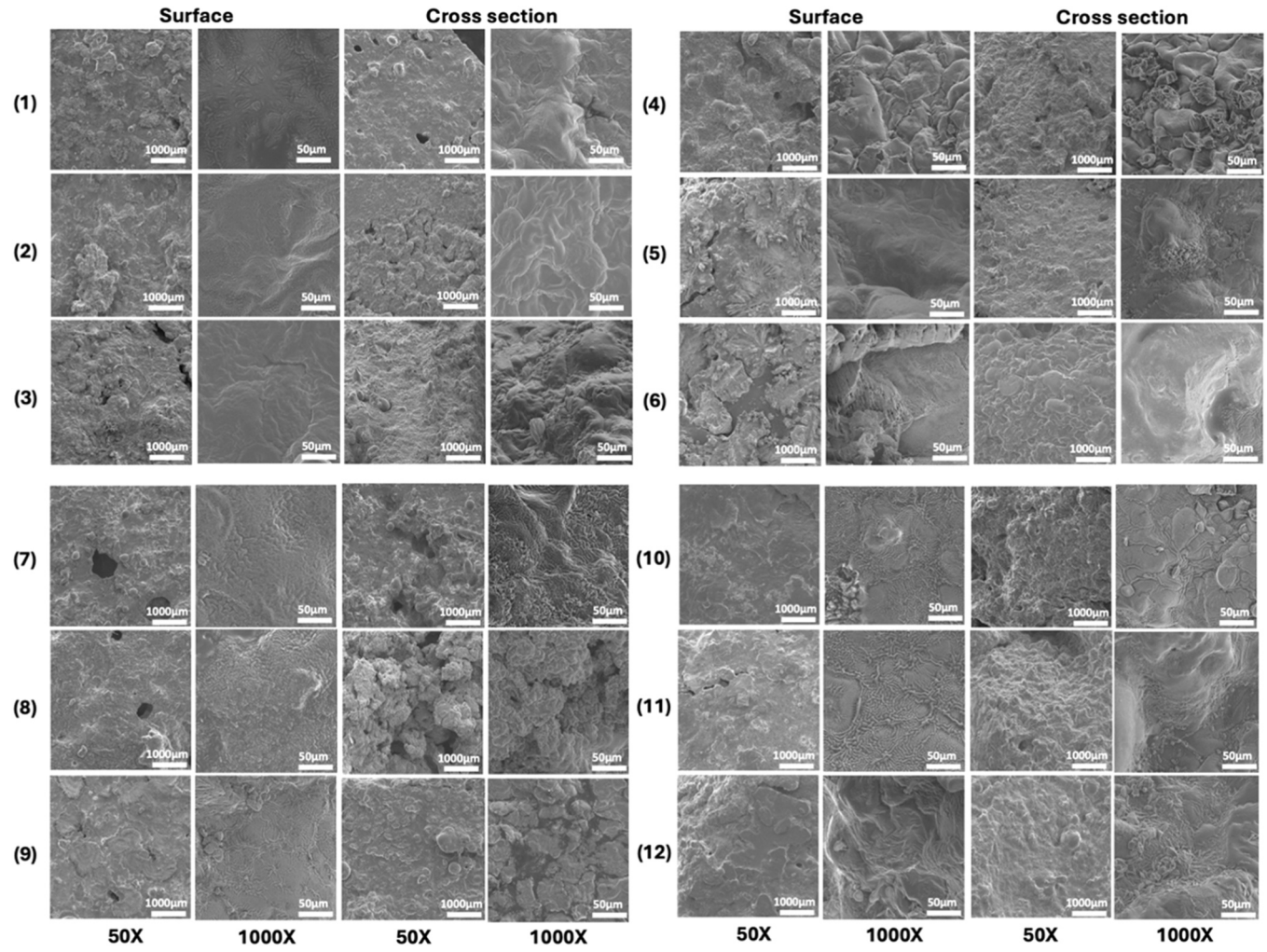

Fig. 8. Morphologies of the films surface and cross section obtained by SEM.

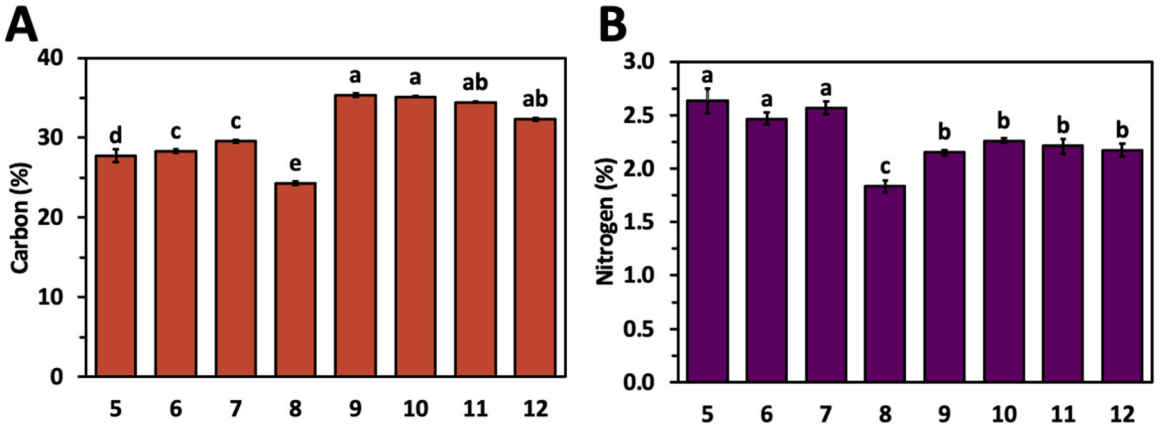

Fig. 9. Percent carbon and nitrogen of different composition films. (A) carbon and (B) nitrogen. Graph represents mean ± SD followed by same letter is not significantly different at $p \leq 0.05$.

be observed in the BSM-10 and BSM-11 films, which showed that lignin did not dissolve properly in the system. This is the reason for the lack of a significant difference in TS and other mechanical properties despite adding lignin. These morphological trends align with starch-lignin composite mulch films, where SEM shows decreased porosity with optimized starch (4–5 %) for enhanced compactness (Huang et al., 2024), and grainy/coarse cross-sections in protein-starch blends due to phase separation (Chen et al., 2025). Similarly, reviews of polysaccharide-protein mulches note increased surface roughness and holes with undissolved lignin, limiting homogeneity (Hassan et al., 2024).

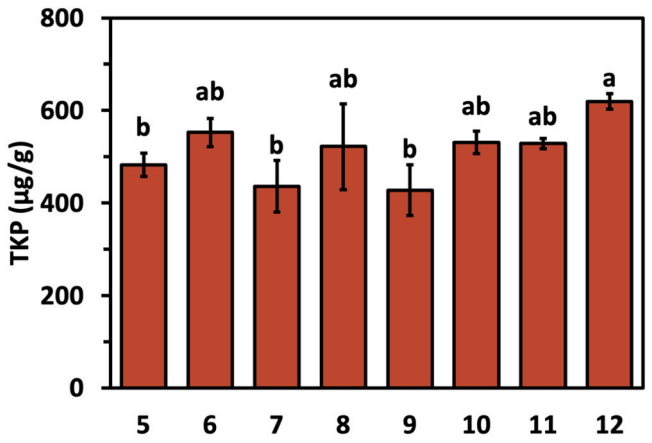

Fig. 10. Total Kjeldahl phosphorus (TKP) of different composition films. Graph represents mean ± SD followed by same letter is not significantly different at $p \leq 0.05$.

3.9. Percentage of carbon and nitrogen

The films with lignin had significantly higher carbon than other films due to its aromatic polymer structure, followed by BSM-6 and BSM-7 films that contained PS ($p < 0.05$). It could be observed from Fig. 9(a) that the lowest C was recorded for BSM-8. The BSM films without lignin had significantly higher N ($p < 0.05$) (Fig. 9b) than films with lignin, because the inclusion of lignin reduced the relative N contribution by increasing the non-nitrogenous fraction. The lowest N was recorded for BSM-8 ($p < 0.05$) which included PP rather than ISP in the formulation. There was no significant difference between the different concentrations of lignin based BSM's N ($p > 0.05$). Similar %C = 40.2–43.5 values were observed in a study on starch-based filler derived from waste tempura flakes, conducted by Yoo et al. (2024), but the N values they reported were significantly lower than ours, as they did not incorporate KL or CFW in their formulations.

3.10. Total Kjeldahl phosphorus

Mineral fertilizers provide essential nutrients for plant growth, of the 17 vital elements, nitrogen, phosphorus, and potassium (NPK) are key (Ao et al., 2013). The TKP content was measured for all the BSM samples. BSM-5 exhibited an average TKP value of 483 µg/g, while BSM-6 showed a higher value of 552 µg/g. BSM-7, 8, and 9 had TKP values of 436, 522, and 428 µg/g, respectively. BSM-10 and 11 recorded 531 µg/g and 528 µg/g, respectively and BSM-12 reached the highest TKP value of 619 µg/g. BSM-12 had significantly greater TKP than other treatments ($p < 0.05$, Fig. 10). There was no significant difference in the TKP values of other BSM samples ($p > 0.05$). These TKP levels align with the study carried out by Ao et al. (2013) on phosphorus-release starch-based mulch films, where TKP ranges 500–650 µg/g in residue-enriched variants, enhancing soil P availability by 20–50 %.

3.11. Ammonia-N and nitrate-N

Ammonia-N was significantly higher in BSM-7 than other treatments. Ammonia-N was lowest for BSM-12, which indicates that as lignin content increased the Ammonia-N decreased (Fig. 11A). The highest value for Nitrate-N was observed for BSM-8, which might be due to the addition of PP into the system rather than ISP. This was significantly higher than the Nitrate-N values of BSM-5, 6 and 7. Also, addition of lignin into the system increased the Nitrate-N values when added more than 0.3 % (w/v). The mean values of Nitrate-N were not significantly different among films with lignin (Fig. 11B).

4. Conclusions

This study demonstrates the potential of BSM formulations as a sustainable alternative for agricultural applications. By incorporating protein–glycerol or protein–glycerol–lignin blends into starch–keratin hydrolysate matrices, we developed twelve BSM films and evaluated their physicochemical, mechanical, and morphological characteristics. Among these, BSM-5 and BSM-12 films exhibited superior mechanical properties and favorable functional attributes compared to other films, including high TS, EB, WA, and nutrient profiles, indicating their strong potential as biodegradable spray-on mulches.

FTIR and TGA analyses confirmed the chemical and thermal stability of the BSM films. SEM imaging revealed that incorporating 4 % starch effectively reduced filler–filler interactions and enhanced matrix densification, thereby improving film integrity. These structural optimizations translated into improved material performance, particularly for BSM-12, which achieved a TS of 23 kPa and an EB of 15.39 %.

Importantly, BSM films are biodegradable and derived from renewable resources, such as CFW, making them a viable circular solution for plastic mulch replacement. Their ability to gradually release nitrogen and maintain structural integrity under varying environmental conditions positions them as a dual-function mulches, serving both as a physical barrier for weed suppression and as a slow-release nitrogen source for plant uptake. Beyond mulching, these BSM formulations could encapsulate pesticides or fertilizers for controlled release, further enhancing their utility in sustainable agriculture.

This research lays the groundwork for advancing circular bioeconomy strategies by valorizing waste streams into high-value, sustainable agricultural inputs. These findings have significant implications for regenerative agriculture, particularly in reducing plastic waste and

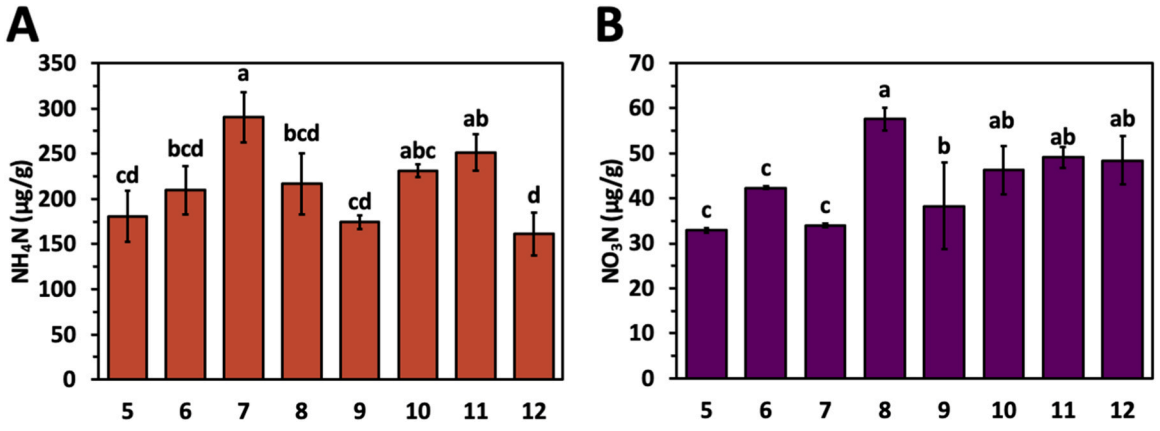

Fig. 11. Ammonia-N and nitrate-N of different composition films. Graph represents mean ± SD followed by same letter is not significantly different at $p \leq 0.05$.

enhancing soil fertility. This study focused on lab-scale characterization, and field performance under variable weather remains untested. Viscosity measurements were conducted at 25 °C, which did not simulate spray conditions (e.g., 40 °C). The BSMs developed here show promise for reinforcement with other polymers or organic fillers to enhance mechanical stability. Future formulations could incorporate other materials, such as gelatin, beeswax, or chitosan nanofibers for improved TS and water resistance. There is a need to develop more sustainable processes to produce CFKH using clean approaches such as enzymatic or subcritical water hydrolysis. To maximize agricultural applicability, future research should focus on field-scale validation under diverse climatic and cropping systems, optimization of formulations for pest resistance, and life cycle assessments to quantify environmental benefits. Integration with precision spraying technologies could further facilitate adoption in commercial agriculture.

CRediT authorship contribution statement

Brown Brandi: Methodology, Investigation, Data curation. **Akram Muhammad:** Writing – original draft, Methodology, Investigation, Formal analysis, Data curation, Conceptualization. **Mark Wilkins:** Writing – review & editing, Supervision, Resources, Project administration, Methodology, Funding acquisition, Conceptualization. **Ozan N. Ciftci:** Writing – review & editing, Supervision, Resources, Project administration, Methodology, Funding acquisition, Conceptualization.

Declaration of Competing Interest

The authors declare that there is no conflict of interest regarding the publication of this article.

Acknowledgements

This work was supported by the National Science Foundation EPSCoR RII Track-2 FEC (Grant no. 2119753).

Data availability

Data will be made available on request.

References

Adhikari, R., Bristow, K.L., Casey, P.S., Freischmidt, G., Hornbuckle, J.W., Adhikari, B., 2016. Preformed and sprayable polymeric mulch film to improve agricultural water use efficiency. Agric. Water Manag. 169 (C), 1–13.

Amin, U., Khan, M.A., Akram, M.E., Al-Tawaha, A.R.M.S., Laishevtcev, A., Shariati, M.A., 2019. Characterization of compisote edible films from aloe vera gel, beeswax and chitosan. Potravina Slovak J. Food Sci. 13 (1), 854–862. https://doi.org/10.5219/1177.

Ao, L., Qin, L., Kang, H., Zhou, Z., Su, H., 2013. Preparation, properties and field application of biodegradable and phosphorus-release films based on fermentation residue. Int. Biodeterior. Biodegrad. 82, 134–140. https://doi.org/10.1016/j.ibiod.2013.02.009.

Azahari, N.A., Othman, N., Ismail, H., 2011. Biodegradation studies of polyvinyl alcohol/corn starch blend films in solid and solution media. J. Phys. Sci. 22.

Basiak, E., Lenart, A., Debeaufort, F., 2017. Effect of starch type on the physico-chemical properties of edible films. Int. J. Biol. Macromol. 98, 348–356. https://doi.org/10.1016/j.ijbiomac.2017.01.122.

Benigno, S.M., Dixon, K.W., Stevens, J.C., 2013. Increasing soil water retention with Native-Sourced mulch improves seedling establishment in postmine Mediterranean sandy soils. Restor. Ecol. 21 (5), 617–626. https://doi.org/10.1111/j.1526–100X.2012.00926.x.

Benito-González, I., López-Rubio, A., Martínez-Sanz, M., 2019. High-performance starch biocomposites with celullose from waste biomass: film properties and retrogradation behaviour. Carbohydr. Polym. 216, 180–188. https://doi.org/10.1016/j.carbpol.2019.04.030.

Bhat, R., Abdullah, N., Din, R.H., Tay, G.-S., 2013. Producing novel sago starch based food packaging films by incorporating lignin isolated from oil palm black liquor waste. J. Food Eng. 119 (4), 707–713. https://doi.org/10.1016/j.jfoodeng.2013.06.043.

Bi, S., Pan, H., Barinelli, V., Eriksen, B., Ruiz, S., Sobkowicz, M., 2021. Biodegradable polyester coated mulch paper for controlled release of fertilizer. J. Clean. Prod. 294, 126348. https://doi.org/10.1016/j.jclepro.2021.126348.

Briassoulis, D., 2006. Mechanical behaviour of biodegradable agricultural films under real field conditions. Polym. Degrad. Stab. 91 (6), 1256–1272. https://doi.org/10.1016/j.polymdegradstab.2005.09.016.

Briassoulis, D., 2007. Analysis of the mechanical and degradation performances of optimised agricultural biodegradable films. Polym. Degrad. Stab. 92 (6), 1115–1132. https://doi.org/10.1016/j.polymdegradstab.2007.01.024.

Briassoulis, D., Giannoulis, A., 2018. Evaluation of the functionality of bio-based plastic mulching films. Polym. Test. 67, 99–109. https://doi.org/10.1016/j.polymertesting.2018.02.019.

Castro-Muñoz, R., Kharazmi, M.S., Jafari, S.M., 2023. Chitosan-based electrospun nanofibers for encapsulating food bioactive ingredients: a review. Int. J. Biol. Macromol. 245, 125424. https://doi.org/10.1016/j.ijbiomac.2023.125424.

Chaparro, J.M., Sheflin, A.M., Manter, D.K., Vivanco, J.M., 2012. Manipulating the soil microbiome to increase soil health and plant fertility. Biol. Fertil. Soils 48 (5), 489–499. https://doi.org/10.1007/s00374–012-0691–4.

Chen, C., Li, Z., Yin, K., Li, L., Zhang, Z., Xu, X., Liu, H., Qing, Y., Li, X., Wu, Y., 2025. Biodegradable liquid slow-release mulch film based on bamboo residue for selenium-enriched crop cultivation. Research. https://doi.org/10.34133/research.0685.

Chen, L., Dai, R., Shan, Z., Chen, H., 2020. Fabrication and characterization of one high-hygroscopicity liquid starch-based mulching materials for facilitating the growth of plant. Carbohydr. Polym. 230, 115582. https://doi.org/10.1016/j.carbpol.2019.115582.

Cuello, J.P., Hwang, H.Y., Gutierrez, J., Kim, S.Y., Kim, P.J., 2015. Impact of plastic film mulching on increasing greenhouse gas emissions in temperate upland soil during maize cultivation. Appl. Soil Ecol. 91, 48–57. https://doi.org/10.1016/j.apsoil.2015.02.007.

Cyras, V.P., Manfredi, L.B., Ton-That, M.-T., Vázquez, A., 2008. Physical and mechanical properties of thermoplastic starch/montmorillonite nanocomposite films. Carbohydr. Polym. 73 (1), 55–63. https://doi.org/10.1016/j.carbpol.2007.11.014 (Scopus.

Dąbrowska, M., Sommer, A., Sinkiewicz, I., Taraszkiewicz, A., Staroszczyk, H., 2022. An optimal designed experiment for the alkaline hydrolysis of feather keratin. Environ. Sci. Pollut. Res. Int. 29 (16), 24145–24154. https://doi.org/10.1007/s11356–021-17649–2.

Dada, O.I., Habarakada Liyanage, T.U., Chi, T., Yu, L., DeVetter, L.W., Chen, S., 2025. Towards sustainable agroecosystems: a life cycle assessment review of soil-biodegradable and traditional plastic mulch films. Environ. Sci. Ecotechnol. 24, 100541. https://doi.org/10.1016/j.ese.2025.100541.

Dang, K.M., Yoksan, R., 2015. Development of thermoplastic starch blown film by incorporating plasticized chitosan. Carbohydr. Polym. 115, 575–581. https://doi.org/10.1016/j.carbpol.2014.09.005.

Datta, D., Halder, G., 2019. Effect of media on degradability, physico-mechanical and optical properties of synthesized polyolefinic and PLA film in comparison with casted potato/corn starch biofilm. Process Safety and Environmental Protection 124, 39–62. https://doi.org/10.1016/j.psep.2019.02.002.

Edhirej, A., Sapuan, S.M., Jawaid, M., Zahari, N.I., 2017. Cassava/sugar palm fiber reinforced cassava starch hybrid composites: physical, thermal and structural properties. Int. J. Biol. Macromol. 101, 75–83. https://doi.org/10.1016/j.ijbiomac.2017.03.045.

Eranda, D.H.U., Chaijan, M., Panpipat, W., Karnjanapratum, S., Cerqueira, M.A., Castro-Muñoz, R., 2024. Gelatin-chitosan interactions in edible films and coatings doped with plant extracts for biopreservation of fresh tuna fish products: a review. Int. J. Biol. Macromol. 280 (Pt 2), 135661. https://doi.org/10.1016/j.ijbiomac.2024.135661.

Ferreira-Filipe, D.A., Paço, A., Duarte, A.C., Rocha-Santos, T., Patrício Silva, A.L., 2021. Are biobased plastics green alternatives?—a critical review. Int. J. Environ. Res. Public Health 18 (15), 7729. https://doi.org/10.3390/ijerph18157729.

Gloeb, E., Irmak, S., Isom, L., Lindquist, J.L., Wortman, S.E., 2023. Biobased sprayable mulch films suppressed annual weeds in vegetable crops. HortTechnology 33 (1), 27–35. https://doi.org/10.21273/HORTTECH05112–22.

Hassan, F., Mu, B., Yang, Y., 2024. Natural polysaccharides and proteins-based films for potential food packaging and mulch applications: a review. Int. J. Biol. Macromol. 261 (Pt 1), 129628. https://doi.org/10.1016/j.ijbiomac.2024.129628.

Hernández-Pinto, F.J., Miranda-Medina, J.D., Natera-Maldonado, A., Vara-Aldama, Ó., Ortueta-Cabranes, M.P., Vázquez Del Mercado-Pardiño, J.A., El-Aidie, S.A.M., Siddiqui, S.A., Castro-Muñoz, R., 2024. Arabinoxylans: a review on protocols for their recovery, functionalities and roles in food formulations. Int. J. Biol. Macromol. 259 (Pt 2), 129309. https://doi.org/10.1016/j.ijbiomac.2024.129309.

Horodytska, O., Valdés, F.J., Fullana, A., 2018. Plastic flexible films waste management – a state of art review. Waste Manag. 77, 413–425. https://doi.org/10.1016/j.wasman.2018.04.023.

Huang, Z., Xu, Z., Chen, C., 2008. Effect of mulching on labile soil organic matter pools, microbial community functional diversity and nitrogen transformations in two hardwood plantations of subtropical Australia. Appl. Soil Ecol. 40 (2), 229–239. https://doi.org/10.1016/j.apsoil.2008.04.009.

Huang, Z., Zhang, Y., Zhang, C., Yuan, F., Gao, H., Li, Q., 2024. Lignin-Based composite film and its application for agricultural mulching. Polymers 16 (17), 2488. https://doi.org/10.3390/polym16172488.

Immirzi, B., Santagata, G., Vox, G., Schettini, E., 2009. Preparation, characterisation and field testing of a biodegradable sodium alginate-based spray mulch. Biosyst. Eng. 102, 461–472. https://doi.org/10.1016/j.biosystemseng.2008.12.008.

Johnston, P., Freischmidt, G., Easton, C.D., Greaves, M., Casey, P.S., Bristow, K.L., Gunatillake, P.A., Adhikari, R., 2017. Hydrophobic-hydrophilic surface switching properties of nonchain extended poly(urethane)s for use in agriculture to minimize soil water evaporation and permit water infiltration. J. Appl. Polym. Sci. 134 (45), 44756. https://doi.org/10.1002/app.44756.

Kurt, A., Kahyaoglu, T., 2014. Characterization of a new biodegradable edible film made from salep glucomannan. Carbohydr. Polym. 104, 50–58. https://doi.org/10.1016/j.carbpol.2014.01.003.

Li, H., Gidley, M.J., Dhital, S., 2019. High-Amylose starches to bridge the "fiber gap": development, structure, and nutritional functionality. Compr. Rev. Food Sci. Food Saf. 18 (2), 362–379. https://doi.org/10.1111/1541–4337.12416.

Lorenzo Santiago, M.A., Rendón Villalobos, J.R., Contreras Ramos, S.M., Pacheco Vargas, G., García Hernández, E., 2024. Biodegradation studies of biobased mulch films reinforced with cellulose from waste mango. Recycling 9 (5), 96. https://doi.org/10.3390/recycling9050096.

Mali, S., Grossmann, M.V.E., García, M.A., Martino, M.N., Zaritzky, N.E., 2006. Effects of controlled storage on thermal, mechanical and barrier properties of plasticized films from different starch sources. J. Food Eng. 75 (4), 453–460. https://doi.org/10.1016/j.jfoodeng.2005.04.031.

Malińska, K., Pudełko, A., Postawa, P., Stachowiak, T., Dróżdż, D., 2022. Performance of biodegradable biochar-added and bio-based plastic clips for growing tomatoes. Materials 15 (20), 7205. https://doi.org/10.3390/ma15207205.

Menossi, M., Cisneros, M., Alvarez, V.A., Casalongué, C., 2021. Current and emerging biodegradable mulch films based on polysaccharide bio-composites. a review. Agron. Sustain. Dev. 41 (4), 53. https://doi.org/10.1007/s13593–021-00685–0.

Method 365.4: Phosphorous, Total (Colorimetric, Automated, Block Digester AA II), n.d.

Mokrejs, P., Svoboda, P., Hrncirik, J., Janacova, D., Vasek, V., 2011. Processing poultry feathers into keratin hydrolysate through alkaline-enzymatic hydrolysis. Waste Manag. Res. 29 (3), 260–267. https://doi.org/10.1177/0734242X10370378.

Nan, W., Yue, S., Huang, H., Li, S., Shen, Y., 2016. Effects of plastic film mulching on soil greenhouse gases (CO2, CH4 and N2O) concentration within soil profiles in maize fields on the Loess Plateau, China. J. Integr. Agric. 15 (2), 451–464. https://doi.org/10.1016/S2095–3119(15)61106–6.

Nordin, N., Othman, S.H., Rashid, S.A., Basha, R.K., 2020. Effects of glycerol and thymol on physical, mechanical, and thermal properties of corn starch films. Food Hydrocoll. 106, 105884. https://doi.org/10.1016/j.foodhyd.2020.105884.

Park, J.W., Im, S.S., Kim, S.H., Kim, Y.H., 2000. Biodegradable polymer blends of poly(L-lactic acid) and gelatinized starch. Polym. Eng. Sci. 40 (12), 2539–2550. https://doi.org/10.1002/pen.11384.

Pelissari, F.M., Grossmann, M.V.E., Yamashita, F., Pined, E.A.G., 2009. Antimicrobial, mechanical, and barrier properties of cassava starch-chitosan films incorporated with oregano essential oil. J. Agric. Food Chem. 57 (16), 7499–7504. https://doi.org/10.1021/jf9002363.

Picuno, P., 2014. Innovative material and improved technical design for a sustainable exploitation of agricultural plastic film. Polym. Plast. Technol. Eng. 53 (10), 1000–1011. https://doi.org/10.1080/03602559.2014.886056.

Qin, D., Ma, Y., Wang, M., Shan, Z., 2024. Study on nutrient carrier of mulch based on hydrogel @SiO2. Polymers 16 (10), 1442. https://doi.org/10.3390/polym16101442.

Ramakrishnan, N., Sharma, S., Gupta, A., Alashwal, B.Y., 2018. Keratin based bioplastic film from chicken feathers and its characterization. Int. J. Biol. Macromol. 111, 352–358. https://doi.org/10.1016/j.ijbiomac.2018.01.037.

Sabatino, L., Iapichino, G., Vetrano, F., Moncada, A., Miceli, A., De Pasquale, C., D'Anna, F., Giurgiulescu, L., 2018. Effects of polyethylene and biodegradable Starch-Based mulching films on eggplant production in a Mediterranean area. Carpathian J. Food Sci. Technol. 10 (3), 81–89.

Sahari, J., Sapuan, S., Zainudin, E.S., Maleque, M., 2014. Physico-chemical and thermal properties of starch derived from sugar palm tree (Arenga pinnata). Asian J. Chem. 26, 955–959. https://doi.org/10.14233/ajchem.2014.15652.

Santamaria, M., Garzon, R., Moreira, R., Rosell, C.M., 2021. Estimation of viscosity and hydrolysis kinetics of corn starch gels based on microstructural features using a simplified model. Carbohydr. Polym. 273, 118549. https://doi.org/10.1016/j.carbpol.2021.118549.

Sanyang, M.L., Sapuan, S.M., Jawaid, M., Ishak, M.R., Sahari, J., 2015. Effect of plasticizer type and concentration on tensile, thermal and barrier properties of biodegradable films based on sugar palm (Arenga pinnata) starch. Polymers 7 (6), 6. https://doi.org/10.3390/polym7061106.

Schettini, E., Sartore, L., Barbaglio, M., Vox, G., 2012. Hydrolyzed protein based materials for biodegradable spray mulching coatings. Acta Hortic. (952), 359–366. https://doi.org/10.17660/ActaHortic.2012.952.45.

Serrano-Ruiz, H., Martin-Closas, L., Pelacho, A.M., 2021. Biodegradable plastic mulches: impact on the agricultural biotic environment. Sci. Total Environ. 750, 141228. https://doi.org/10.1016/j.scitotenv.2020.141228.

Siddiqui, S.A., Yang, X., Deshmukh, R.K., Gaikwad, K.K., Bahmid, N.A., Castro-Muñoz, R., 2024. Recent advances in reinforced bioplastics for food packaging—a critical review. Int. J. Biol. Macromol. 263 (Pt 2), 130399. https://doi.org/10.1016/j.ijbiomac.2024.130399.

Sokombela, A., Ndhlala, A.R., Bopape-Mabapa, M.P., Eiasu, B.K., Mpai, S., Nyambo, P., 2025. Colored plastic mulch impacts on soil properties, weed density and vegetable crop productivity: a meta-analysis. Sci. Rep. 15 (1), 31891. https://doi.org/10.1038/s41598–025-17237–1.

Spalding, R.F., Kitchen, L.A., 1988. Nitrate in the intermediate vadose zone beneath irrigated cropland. Groundw. Monit. Remediat. 8 (2), 89–95. https://doi.org/10.1111/j.1745–6592.1988.tb00994.x.

Stasi, E., Giuri, A., Ferrari, F., Armenise, V., Colella, S., Listorti, A., Rizzo, A., Ferraris, E., Esposito Corcione, C., 2020. Biodegradable carbon-based ashes/maize starch composite films for agricultural applications. Polymers 12 (3), 524. https://doi.org/10.3390/polym12030524.

Suppakul, P., Chalernsook, B., Ratisuthawat, B., Prapasitthi, S., Munchukangwan, N., 2013. Empirical modeling of moisture sorption characteristics and mechanical and barrier properties of cassava flour film and their relation to plasticizing–antiplasticizing effects. LWT - Food Sci. Technol. 50 (1), 290–297. https://doi.org/10.1016/j.lwt.2012.05.013.

Talja, R.A., Helén, H., Roos, Y.H., Jouppila, K., 2007. Effect of various polyols and polyol contents on physical and mechanical properties of potato starch-based films. Carbohydr. Polym. 67 (3), 288–295. https://doi.org/10.1016/j.carbpol.2006.05.019.

Tofanelli, M.B.D., Wortman, S.E., 2020. Benchmarking the agronomic performance of biodegradable mulches against polyethylene mulch film: a meta-analysis. Agronomy 10 (10), 1618. https://doi.org/10.3390/agronomy10101618.

Tongdeesoontorn, W., Mauer, L.J., Wongruong, S., Sriburi, P., Rachtanapun, P., 2012. Mechanical and physical properties of cassava starch-gelatin composite films. Int. J. Polym. Mater. Polym. Biomater. 61 (10), 778–792. https://doi.org/10.1080/00914037.2011.610049.

Torres, F.G., Troncoso, O.P., Torres, C., Díaz, D.A., Amaya, E., 2011. Biodegradability and mechanical properties of starch films from andean crops. Int. J. Biol. Macromol. 48 (4), 603–606. https://doi.org/10.1016/j.ijbiomac.2011.01.026.

Virtanen, S., Chowreddy, R.R., Irmak, S., Honkapää, K., Isom, L., 2017. Food industry co-streams: potential raw materials for biodegradable mulch film applications. J. Polym. Environ. 25 (4), 1110–1130. https://doi.org/10.1007/s10924–016-0888-y.

Wang, K., Wang, C., Chen, M., Misselbrook, T., Kuzyakov, Y., Soromotin, A., Dong, Q., Feng, H., Jiang, R., 2022. Effects of plastic film mulch biodegradability on nitrogen in the plant-soil system. Sci. Total Environ. 833, 155220. https://doi.org/10.1016/j.scitotenv.2022.155220.

Wang, S., Li, C., Copeland, L., Niu, Q., Wang, S., 2015. Starch retrogradation: a comprehensive review. Compr. Rev. Food Sci. Food Saf. 14 (5), 568–585. https://doi.org/10.1111/1541–4337.12143.

Woods, S.R., Fehmi, J.S., Backer, D.M., 2012. An assessment of revegetation treatments following removal of invasive Pennisetum ciliare (buffelgrass). J. Arid Environ. 87, 168–175. https://doi.org/10.1016/j.jaridenv.2012.06.009.

Yin, M., Li, Y., Xu, Y., Zhou, C., 2018. Effects of mulches on water use in a winter wheat/summer maize rotation system in Loess Plateau, China. J. Arid Land 10 (2), 277–291. https://doi.org/10.1007/s40333–018-0092–0.

Yoo, S., Lee, S., Kang, S.-W., Ahn, K.-H., 2024. Upcycling waste tempura flake-derived starch powder as an environment-friendly polymer matrix filler for thermoplastic starch compounds. BioResources 19 (1), 1394–1409.

Youkhana, A., Idol, T., 2009. Tree pruning mulch increases soil C and N in a shaded coffee agroecosystem in hawaii. Soil Biol. Biochem. 41 (12), 2527–2534. https://doi.org/10.1016/j.soilbio.2009.09.011.

Zadeh, E.M., O'Keefe, S.F., Kim, Y.-T., 2018. Utilization of lignin in biopolymeric packaging films. ACS Omega 3 (7), 7388–7398. https://doi.org/10.1021/acsomega.7b01341.

Zhang, W., Azizi-Lalabadi, M., Roy, S., Salim, S.A., Castro-Muñoz, R., Jafari, S.M., 2023. Maillard-reaction (glycation) of biopolymeric packaging films; principles, mechanisms, food applications. Trends Food Sci. Technol. 138, 523–538. https://doi.org/10.1016/j.tifs.2023.06.026.

Zhang, X., You, S., Tian, Y., Li, J., 2019. Comparison of plastic film, biodegradable paper and bio-based film mulching for summer tomato production: soil properties, plant growth, fruit yield and fruit quality. Sci. Hortic. 249, 38–48. https://doi.org/10.1016/j.scienta.2019.01.037.